HHS Public Access

Author manuscript

Neurobiol Aging. Author manuscript; available in PMC 2017 August 13.

Published in final edited form as:

Neurobiol Aging. 2017 March ; 51: 141–147. doi:10.1016/j.neurobiolaging.2016.12.011.

Retinal thinning is uniquely associated with medial temporal lobe atrophy in neurologically normal older adults

Kaitlin B. Casaletto[a,*,1], **Michael E. Ward**[a,b,1], **Nicholas S. Baker**[a], **Brianne M. Bettcher**[c,d], **Jeffrey M. Gelfand**[a], **Yaqiao Li**[e], **Robert Chen**[a], **Shubir Dutt**[a], **Bruce Miller**[a], **Joel H. Kramer**[a], and **Ari J. Green**[a]

[a]Department of Neurology, University of California, San Francisco, CA, USA

[b]National Institute of Neurological Disorders and Stroke, National Institutes of Health, Bethesda, MD, USA

[c]Department of Neurosurgery, Rocky Mountain Alzheimer's Disease Center, University of Colorado, Denver Anschutz Medical Center, Aurora, CO, USA

[d]Department of Neurology, Rocky Mountain Alzheimer's Disease Center, University of Colorado, Denver Anschutz Medical Center, Auorora, CO, USA

[e]Gladstone Institute of Neurological Disease, Department of Neurology, University of California, San Francisco, CA, USA

Abstract

Given the converging pathologic and epidemiologic data indicating a relationship between retinal integrity and neurodegeneration, including Alzheimer's disease (AD), we aimed to determine if retinal structure correlates with medial temporal lobe (MTL) structure and function in neurologically normal older adults. Spectral-domain optical coherence tomography, verbal and visual memory testing, and 3T-magnetic resonance imaging of the brain were performed in 79 neurologically normal adults enrolled in a healthy aging cohort study. Retinal nerve fiber thinning and reduced total macular and macular ganglion cell volumes were each associated with smaller MTL volumes (ps < 0.04). Notably, these markers of retinal structure were not associated with primary motor cortex or basal ganglia volumes (regions relatively unaffected in AD) (ps > 0.70), or frontal, precuneus, or temporoparietal volumes (regions affected in later AD Braak staging ps > 0.20). Retinal structure was not significantly associated with verbal or visual memory consolidation performances (ps > 0.14). Retinal structure was associated with MTL volumes, but not memory performances, in otherwise neurologically normal older adults. Given that MTL atrophy is a neuropathological hallmark of AD, retinal integrity may be an early marker of ongoing AD-related brain health.

[*]Corresponding author at: Memory and Aging Center, University of California, San Francisco, 675 Nelson Rising Lane, San Francisco, CA 94158, USA. Tel.: 415-353-8365; fax: 415-476-1816. kaitlin.casaletto@ucsf.edu.

[1]These authors contributed equally to the manuscript.

Disclosure statement

The remaining authors report no conflicts of interest to disclose.

Keywords

Aging; Alzheimer's disease; Optical coherence tomography; Neurodegenerative disease; Dementia; Retinal imaging

1. Introduction

Epidemiologic and pathologic data demonstrate a relationship between age-related neurodegenerative diseases of the retina (e.g., open angle glaucoma) and neurodegenerative diseases of the brain (Helmer et al., 2013; Sivak, 2013). For example, individuals with late-stage Alzheimer's disease (AD) have 5 times higher prevalence of glaucoma than nondemented adults (Bayer et al., 2002; Tamura et al., 2006), and postmortem studies demonstrate substantial retinal ganglion cell loss and optic nerve atrophy in AD (Blanks et al., 1996b; Hinton et al., 1986). In addition, amyloid beta plaques are evidenced in the retinas of postmortem AD patients and in vivo AD transgenic mice, indicating similar pathologies in both the brain and retina in AD (Koronyo-Hamaoui et al., 2011).

Knowing when the retina might become involved during neurodegeneration (i.e., preclinical, prodromal, vs. clinical) is not well understood but has important clinical diagnostic implications. Retinal imaging studies using optical coherence tomography (OCT) in humans demonstrate retinal nerve fiber layer thinning in both mild AD and amnestic mild cognitive impairment (Berisha et al., 2007; Paquet et al., 2007), and these changes may correlate with AD duration and global cognitive status (i.e., mini-mental state examination) (Garcia-Martin et al., 2016). Early retinal changes have also been observed in humans and mouse models of other neurodegenerative diseases, including multiple sclerosis, frontotemporal lobar degeneration, Parkinson's disease, and Huntington's disease, suggesting retinal neurons may be a particularly vulnerable cell population (Altintas et al., 2008; Gelfand et al., 2012; Hafler et al., 2014; Schon et al., 2012; Ward et al., 2014). Identifying the earliest point(s) of neurodegeneration in the retina relative to those in the brain will help advance noninvasive, early detection, and monitoring techniques for at-risk individuals.

We examined the relationship between classic features of AD progression (memory consolidation and medial temporal lobe [MTL] volumes) (Caselli et al., 2014; Schacter, 1999; Squire et al., 2004) and OCT retinal imaging in neurologically normal older adults. We hypothesized that reduced retinal integrity would be associated with reduced memory consolidation and MTL volumes in normal aging.

2. Methods

2.1. Participants

Seventy-nine neurologically normal older adults (ages, 63–91) were recruited as part of a healthy aging study from the Memory and Aging Center at the University of California, San Francisco. Inclusion criteria included neurologic and neuropsychological examination within normative standards per consensus research criteria (McKhann et al., 2011), no major memory concerns or a diagnosed memory condition, and ability to independently complete activities of daily living as operationalized by a Clinical Dementia Rating of 0 (determined

via interviews with participant study partner informants). Participants were additionally screened for ophthalmologic conditions that could potentially impact the retina-brain relationship under study (e.g., preexisting glaucoma, age-related macular degeneration), which included significant myopia (i.e., corrections for distance >6 diopters). By excluding high myopia, we aimed to limit the effect of retinal axial length in our brain-retina analyses. All participants provided written informed consent, and the UCSF Committee on Human Research approved the study protocol.

2.2. Optical coherence tomography

Spectral-domain OCT was performed by a trained technician (NSB) and reviewed by a neuro-ophthalmologist (AJG) in the UCSF Sandler Neuroscience Clinical Research Unit using a single Spectralis OCT system (Heidelberg Engineering). Retinal nerve fiber layer (RNFL) thicknesses were obtained from peripapillary B-scans placed at a 3.4-mm radial distance away from the center of the optic nerve head. Macular volumes were calculated by integrating 19 horizontal B-scans and measured as the volume in a circular region centered on the fovea with a diameter of 3.45 mm. Laboratory standards for OCT scans, including cutoffs for quality and automatic real-time numbers, were adhered to ensure data reliability. Specifically, we only included peripapillary RNFL scans with a quality number of at least 20 and automatic real-time number of at least 40, and macular volume scans with a minimum average quality of 25 and real-time number of 16. The quality number is a metric for signal-to-noise ratio, whereas the automatic real-time number indicates the amount of B-scans averaged to produce the final image. Images were reviewed for retinal pathologies by a neuro-ophthalmologist (AJG). We excluded patients with abnormalities that would have given biased readings for retinal layer thickness. For example, an individual with epiretinal membrane will appear as if s/he has thicker RNFL, but the added thickness is in fact the epiretinal membrane on top of the RNFL. Given that our hypotheses of interest pertained to the relationships between retinal structure and brain structure and function, data from patients with such extraretinal abnormalities would be misleading and were therefore excluded. In total, n = 4 participants were excluded for such retinal abnormalities. Given its high prevalence in normal aging and to increase our generalizability, participants with a history of cataract surgeries were included in analyses (14/79, 17.8% reported history of cataract surgery). Fig. 1 illustrates each type of retinal OCT scan.

2.3. Neuroimaging

Magnetic resonance imaging (MRI) scans were obtained using a 3-Tesla Magnetom VISION system (Siemens, Iselin, NJ, USA). T1-weighted whole-brain images were acquired with a volumetric magnetization prepared rapid gradient-echo sequence (MPRAGE, repetition time [TR]/echo time [TE]/inversion time [TI] = 10/4/300 ms) with 15-degree flip angle, coronal orientation perpendicular to the double spin-echo sequence, 1.0 × 1.0-mm in-plane resolution and 1.5-mm slab thickness.

2.3.1. Freesurfer analyses—T1 MPRAGE structural images were subsequently analyzed using Freesurfer version 5.1, which is freely available online for download (http://surfer.nmr.mgh.harvard.edu/). Freesurfer is a structural MRI analysis program that segments white matter and tessellates gray and white matter surfaces. The technical details of

Freesurfer have been described and validated extensively elsewhere (Dale et al., 1999; Fischl et al., 1999; Fischl et al., 2001; Segonne et al., 2004). In brief, this is completed by removing nonbrain tissue with a hybrid watershed/surface deformation procedure (Fischl et al., 2001) and intensity normalization (Segonne et al., 2004), followed by automated Talairach transformation and segmentation into cortical and subcortical gray and white matter. Total intracranial volume was calculated via an atlas normalization procedure (Buckner et al., 2004). Once the cortical models were completed, the surfacing algorithm corrected for topological defects, completed surface inflation, registered to a spherical atlas, parcelated cerebral cortex into regions of interest based on gyral and sulcal structure, and created surface-based data that used both intensity and continuity information from the entire 3-dimensional MR volume. Finally, images were individually quality checked for accuracy of segmentation, and manual edits were made as needed to correct common geometric inaccuracies in white matter and pial surfaces.

The primary region of interest was the MTL (sum of bilateral entorhinal, parahippocampal, and hippocampal volumes). To determine the specificity of the relationship between the retina and MTL, we also examined areas affected in later AD pathogenesis (bilateral temporoparietal cortex [sum of superior temporal and inferior parietal lobules], precuneus, and posterior cingulate volumes), areas affected more generally in aging (bilateral midfrontal volumes), and areas less susceptible to aging or AD (bilateral basal ganglia [sum of bilateral caudate, pallidum, accumbens, putamen] and primary motor cortex) (Rabinovici et al., 2007).

2.4. Neuropsychological episodic memory testing

As measures of MTL function, all participants were administered a measure of verbal episodic memory, the California Verbal Learning Test–second edition (CVLT-II) (Delis et al., 1987, 2000), and visual episodic memory, the Behavioral Pattern Separation Test (BPS-O) (Kirwan and Stark, 2007).

On the CVLT-II, participants were given 16 words to recall across 5 learning trials. After an interference trial, participants were asked to recall the initial list both immediately and after a 20-minute delay (long delay). We examined the total number of words recalled after the long delay (range, 0–16 words), and in our regression models, controlled for the number of words recalled by trial 5 to adjust for baseline immediate recall.

The BPS-O is a computer-based task of visual pattern separation recognition (ability to differentiate novel yet similar information from previously learned information). On the BPS-O, participants were first shown a set of 40 stimulus items and instructed to indicate, using a keyboard press, if each item was an “indoor” or “outdoor” object. After a 10-minute delay, participants were then shown a set of 120 items: 40 of the original items, 40 novel items, and 40 items that were similar to the original items. Participants were instructed to identify each of these items as “old”, “new”, or “similar”, respectively. Stimuli were presented for 2-second duration and were self-paced (0.5-ms interstimulus interval minimum). BPS-O response bias was calculated as the difference between the rate of “similar” responses given to the lure items minus the “similar” responses given to the foil items, consistent with previously reported literature (Stark et al., 2013). The total percent of

correctly identified items at the delay was analyzed as the primary outcome (i.e., total correct/total trials; possible range: 0%–100%), controlling for response bias. The BPS-O demonstrates robust activation with the MTL in functional MRI paradigms (Law et al., 2005; Yassa et al., 2011) and has been validated to detect age-related memory changes in older adults (Yassa et al., 2011) and hippocampal specific injury (Kirwan et al., 2012).

2.5. Statistical analyses

Multivariable linear regression models were conducted to examine associations between OCT retinal indices (i.e., RNFL thickness, total macular volume, macular ganglion cell volume) and cortical volumes adjusting for intracranial volume, age, and sex. We also explored models additionally adjusting for education. RNFL thickness was calculated by averaging the total peripapillary RNFL value from both eyes of each individual. Similarly, total macular volumes and macular ganglion cell volumes were calculated by averaging the values from both eyes of each individual. Medial temporal lobe volumes were calculated by summing the left and right sides. Associations with, also summed sides, were analyzed reference.

We additionally conducted multivariable linear regression models examining associations between OCT retinal indices (i.e., RNFL thickness, total macular volume, and macular ganglion cell volume) and MTL function using the CVLT-II–delayed recall index (previously described) and the BPS-O, adjusting for age and sex.

Finally, all models were replicated examining OCT retinal indices from the worst eye (e.g., eye with greater level of RNFL thinning), which demonstrated an identical pattern of results.

All analyses were conducted using JMP Pro12 (SAS) software.

3. Results

Of the 79 neurologically normal adults enrolled, the mean age was 76.0 (standard deviation = 5.5) years, 54.5% were women, and all were white (Table 1). The mean education level was 17.6 (standard deviation = 2.0) years, and the median MMSE was 29.5 (interquartile range: 28–30).

3.1. RNFL thinning is associated with reduced MTL volumes

RNFL thinning was associated with smaller medial temporal volumes ($\beta = 0.31$, $p = 0.006$; Table 2). As a comparison, RNFL thinning was not associated with temporoparietal ($\beta = 0.10$), precuneus ($\beta = 0.13$), posterior cingulate ($\beta = 0.11$), midfrontal ($\beta = 0.15$), primary motor cortex ($\beta = 0.04$), or basal ganglia ($\beta = 0.01$) volumes (ps > 0.10).

3.2. Reductions in macular structure are sensitive to integrity of the MTL

Within the retina, total macular volumes were positively associated with MTL volumes ($\beta = 0.23$, $p = 0.04$). Specifically, reduced macular ganglion cell layer volumes were associated with smaller MTL volumes ($\beta = 0.30$, $p = 0.009$). In contrast, neither total macular volumes nor macular ganglion cell volumes were associated with temporoparietal (macula $\beta = 0.07$; macular ganglion $\beta = 0.01$), precuneus (macula $\beta = -0.15$; macular ganglion $\beta = 0.06$),

posterior cingulate (macula β = −0.05; macular ganglion β = 0.02), midfrontal (macula β = 0.08; macular ganglion β = 0.04), primary motor cortex (macula β = 0.01; macular ganglion β = −0.03), or basal ganglia (macula β = −0.08; macular ganglion β = 0.02) volumes (ps > 0.20).

Given that educational attainment can be associated with brain development, we explored models examining the relationship between retinal and MTL structure adjusting for education. Neither retina or MTL was significantly associated with educational levels at α < 0.05, and all effects were minimal (RNFL r = 0.06; total macular volume r = 0.15; macular ganglion r = 0.05; MTL volume r = 0.10). When included in the models, RNFL and macular ganglion cell volumes remained significantly associated with MTL volumes (RNFL β = 0.30; macular ganglion β = 0.32, ps < 0.01); however, the effect between total macular volume and MTL volumes attenuated slightly (β = 0.19, $p = 0.10$). Given our modest sample size and the lack of meaningful association between education and total macular volume invariably, this attenuated effect may represent lack of power and possible type II error.

3.3. RNFL thinning and macular volumes are not associated with delayed recall in neurologically normal older adults

RNFL thinning, total macular volumes, and macular ganglion cell volumes were not significantly associated with either verbal (RNFL β = 0.06, macula β = 0.09, and macular ganglion β = 0.04) or visual (RNFL β = 0.11, macula β = −0.01, macular ganglion β = 0.02) memory consolidation performance (ps > 0.20). These models remained nonsignificant after additionally adjusting for education (ps > 0.05). Notably, performances on both verbal and visual delayed recall tasks fell within the normal range on published normative scores of healthy older adults (Delis et al., 2000; Yassa et al., 2011) (see Table 1).

The relationship between the memory consolidation and the MTL is well established (Squire, 2004; Squire et al., 2004). Therefore, as a means of comparison for our retinal findings and to support the construct validity of our memory measures, we also examined the relationship between verbal and visual memory performance and MTL volumes, adjusting for age, sex, and total intracranial volumes. Measures of memory consolidation demonstrated modest associations with MTL volumes (verbal memory β = 0.47; visual memory β = 0.11), although these were relatively larger than the overall associations observed between retinal structure and memory performance.

3.4. Post hoc analyses

3.4.1. Retinal structure is associated with entorhinal volumes within the MTL

—To better understand which structures within the MTL may be most strongly linked to the retina in neurologically normal adults, we explored associations between each of the retinal structures (RNFL, macular volumes, and macular ganglion volumes) and areas of the MTL, including hippocampal, entorhinal, and parahippocampal volumes (covarying for age, sex, and total intracranial volumes). Reduced entorhinal volumes were significantly associated with RNFL thinning (β = 0.32, $p = 0.02$), smaller total macular volumes (β = 0.38, $p = 0.005$), and reduced macular ganglion cell volume (β = 0.44, $p = 0.002$). On the other hand,

hippocampal volumes were not significantly associated with any of the retinal structures (β range = 0.08–0.25, ps > 0.05), and smaller parahippocampal volumes were only significantly associated with RNFL thinning (β = 0.31, $p = 0.04$) but not total macular (β = 0.21) or macular ganglion cell (β = 0.19) volumes (ps > 0.10).

4. Discussion

As an extension of the brain, the retina shows structural and pathologic changes associated with certain neurodegenerative diseases; yet, our understanding of how or if these processes develop in neurologically normal brains, potentially before the onset of pathology, is not well understood. Our study demonstrates a novel association between retinal structure and MTL atrophy in neurologically normal older adults. Specifically, indicators of both retinal axonal thinning (i.e., RNFL) and neuronal cell loss (i.e., macular ganglion cells) were associated with smaller current MTL cortices; more precisely, these relationships appeared to be primarily driven by associations between retinal and entorhinal volumes. Importantly, the observed relationships were unique to the MTL and were not evident among other brain regions associated with general aging or even in areas affected in later AD pathology stages (e.g., temporoparietal junction, precuneus), suggesting high specificity of the relationship of the retina to neural systems involved in memory rather than reflective of global atrophy. Given that degeneration of the MTL, beginning in the entorhinal cortex, is a hallmark feature of typical AD (Albert et al., 2011; Rabinovici et al., 2007) and prodromal AD, our data suggest that the unique neuroanatomic associations between retinal structure and MTL in these clinically normal older adults may even reflect early AD-related processes.

We did not observe a significant association between retinal integrity and verbal or visual episodic memory performances, which may further support the notion that retinal involvement may occur early in the preclinical stages of AD. Although impaired memory consolidation is a prominent clinical feature of AD and is directly associated with MTL integrity, measureable degeneration of MTL structure occurs prior to the onset of clinical neurocognitive dysfunction (Bateman et al., 2012; Jack et al., 2013). Our sample of older adults was neurologically unimpaired and performed within normal expectations on both memory measures. The observed association between retinal structure and MTL volumes but not memory performances may therefore indicate concurrent degeneration of the retina and brain that precedes measurable clinical cognitive changes.

These findings build on prior work demonstrating associations between retinal changes and AD-related brain processes (Sivak, 2013) and extend the literature into neurologically normal older adults. For example, recent work linked retinal thinning to temporal as well as occipital lobe structure among older adults with mild cognitive impairment (Ong et al., 2015). In addition, Helmer et al. (Helmer et al., 2013) prospectively showed an increased risk of incident dementia in older adults with glaucoma at baseline. Our results suggest that these early retinal changes may in fact be associated with ongoing brain degeneration before the onset of clinical cognitive symptoms or dementia. Similarly, although greater RNFL thinning and retinal neuronal cell loss is observed in amnestic MCI and AD (Blanks et al., 1996b; Paquet et al., 2007), we demonstrate that this relationship occurs in the absence of overt symptoms of cognitive dysfunction.

Despite being inextricably linked within the central nervous system, the pathophysiology of AD-related brain structures with the retina is not clear. Our study demonstrated that both axonal (i.e., nerve fiber layer) and ganglionic cell body reductions in the retina were associated with MTL volumes, congruent with prior work demonstrating up to 50% retinal ganglion cell loss in AD (Blanks et al., 1996a; Blanks et al., 1996b; Paquet et al., 2007). Taken together, these findings suggest that pathologic changes occur directly in the retina and central visual pathways and that these changes are not specific to axonal injury. Degeneration of the retina in AD may be cell autonomous, occurring in retinal neurons independently of concurrent degeneration elsewhere in the central nervous system. Alternatively, retinal degeneration in AD may be noncell autonomous, occurring through trans-synaptic mechanisms.

Given the link between retinal and early AD-associated brain structure (MTL, specifically entorhinal cortex) in our neurologically normal older adults and prior work identifying neurodegenerative changes in the retina in AD, retinal structure may represent an early biomarker of AD and possibly other neurodegenerative diseases. Although it is unclear if amyloid beta plaques or tau neurofibrillary tangles play a role in the heightened risk for retinal neuronal loss observed in AD (Koronyo-Hamaoui et al., 2011; Lu et al., 2013; Perez et al., 2009; Schon et al., 2012), future work linking neural amyloidosis to changes in the retina would help support the link between the retina and AD-specific pathogenesis. Retinal-based imaging may be particularly well positioned as a noninvasive technique for early detection and monitoring. Given the cost-prohibitive nature of amyloid imaging for presymptomatic AD risk of large-scale utilization of CSF biomarkers in otherwise asymptomatic individuals due to the invasiveness of lumbar puncture, the development of low-cost and noninvasive screens to identify individuals at-risk for AD are greatly needed. In particular, techniques that may be sensitive to identify AD processes before the onset of clinical symptoms are critical as early intervention therapies and preventative approaches may be necessary to effectively modify the disease course. OCT of the retina is a noninvasive, cost-effective technique that may be useful for preclinical detection of neurodegenerative disease. Continued efforts advancing our understanding and application of OCT and the role of the retina in neurodegeneration are therefore of high clinical relevance.

Our study also has several limitations for consideration. Given the cross-sectional nature of our data, we were unable to examine if and how the retina and brain change together over time and the temporal order of these changes (i.e., retina before brain or vice versa). In addition, it is unclear from our data if the associations between retinal and MTL structures are in fact related to ongoing changes versus stable relationships. Future longitudinal studies beginning retinal measurements in early age as well as in preclinical older adults who convert to MCI and AD are needed to determine how retinal degeneration may directly relate to brain degeneration. However, ours represent the first data examining retinal imaging in relation to a neuroanatomic marker in neurologically normal older adults and begin to extend the literature across the lifespan. We do not currently have amyloid imaging data or CSF biomarkers available in this sample, which would aid in determining how retinal imaging may correlate more directly with AD proteinopathy, and whether our findings were driven by individuals who were amyloid positive. Although degradation of the MTL is

associated with prodromal AD, Aβ pathology may be an even earlier indicator of AD processes (Jack et al., 2013); therefore, determining the relationship between retinal structure and early brain Aβ levels would help determine the sensitivity of retinal imaging as a preclinical AD biomarker. In addition, although these data were not collected, greater axial lengths (distance from cornea to the fovea) may be associated with increased retinal thinning (Szigeti et al., 2015). As reported in Section 2, we excluded participants with significant myopia (corrected for distance >6 diopters) to minimize the effects of axial lengths in our analyses. However, given that they commonly increase with age, axial lengths may attenuate the relationship between retinal structure and brain measurements. Specifically, larger axial lengths would introduce noise that would make finding an association between retinal and brain structure more difficult. Given that we demonstrate significant retinal-brain associations, it is less likely that axial length/myopia is playing a significant role although their inclusion in future works may be considered. Finally, the inclusion criteria of our sample precluded clinical evidence of current or past neurological dysfunction and intact performance on a cognitive screen. Nevertheless, although participants were neurologically normal at our study visit, it is possible that some may have undetected neurological pathology (e.g., white matter or subtle cognitive changes). Again, examination of these processes in younger adults and other preclinical samples will help in clarifying when retinal integrity may begin reflecting brain-related structure and, potentially, pathology.

5. Conclusions

Reduced retinal structure, including indicators of axonal and cell body integrity, was associated with only smaller MTL volumes but not other age-related brain regions or memory consolidation in a cohort of otherwise neurologically normal older adults. These data support that the retina demonstrates concurrent relationships with AD-related brain structures, and as such, may point to noninvasive retinal imaging techniques (e.g., OCT) as novel screeners for AD-related neurodegeneration. Future work is needed to further examine the role of the retina in neurodegenerative processes across the lifespan and in parallel with other neurodegenerative biomarkers (e.g., Aβ, tau, inflammation). By elucidating the relationship between neurodegenerative processes in the retina and the brain, we may come to a better understanding of the underlying pathobiology of diseases like AD.

Acknowledgments

This study was supported by NIH-NIA grants NIA 1R01AG032289 (principal investigator (PI): Kramer), R01AG048234 (PI: Kramer) and UCSF ADRC P50 AG023501. Our work was also supported by Larry L. Hillblom Network Grant for the Prevention of Age-Associated Cognitive Decline 2014-A-004-NET (PI: Kramer) and National Center for Advancing Translational Sciences of the NIH under Award Number KL2TR000143 (JMG; PI: Gelfand).

J. G. reports receiving personal compensation for consulting on a scientific advisory board for Medimmune and for Genentech; personal compensation for medical legal consulting; research support to UCSF from Quest Diagnostics for development of a dementia care pathway and Genentech and MedDay for clinical trials.

References

Albert MS, DeKosky ST, Dickson D, Dubois B, Feldman HH, Fox NC, Gamst A, Holtzman DM, Jagust WJ, Petersen RC, Snyder PJ, Carrillo MC, Thies B, Phelps CH. The diagnosis of mild cognitive impairment due to Alzheimer's disease: recommendations from the National Institute on

Aging-Alzheimer's Association workgroups on diagnostic guidelines for Alzheimer's disease. Alzheimers Dement. 2011; 7:270–279. [PubMed: 21514249]

Altintas O, Iseri P, Orzkan B, Caglar Y. Correlation between retinal morphological and functional findings and clinical severity in Parkinson's disease. Documenta Ophthalmologica. 2008; 116:137–146. [PubMed: 17962989]

Bateman RJ, Xiong C, Benzinger TL, Fagan AM, Goate A, Fox NC, Marcus DS, Cairns NJ, Xie X, Blazey TM, Holtzman DM, Santacruz A, Buckles V, Oliver A, Moulder K, Aisen PS, Ghetti B, Klunk WE, McDade E, Martins RN, Masters CL, Mayeux R, Ringman JM, Rossor MN, Schofield PR, Sperling RA, Salloway S, Morris JC. Dominantly Inherited Alzheimer Network. Clinical and biomarker changes in dominantly inherited Alzheimer's disease. N. Engl. J. Med. 2012; 367:795–804. [PubMed: 22784036]

Bayer AU, Ferrari F, Erb C. High occurrence rate of glaucoma among patients with Alzheimer's disease. Eur. Neurol. 2002; 47:165–168. [PubMed: 11914555]

Berisha F, Feke GT, Trempe CL, McMeel JW, Schepens CL. Retinal abnormalities in early Alzheimer's disease. Invest. Ophthalmol. Vis. Sci. 2007; 48:2285–2289. [PubMed: 17460292]

Blanks JC, Schmidt SY, Torigoe Y, Porrello KV, Hinton DR, Blanks RH. Retinal pathology in Alzheimer's disease. II. Regional neuron loss and glial changes in GCL. Neurobiol. Aging. 1996a; 17:385–395. [PubMed: 8725900]

Blanks JC, Torigoe Y, Hinton DR, Blanks RH. Retinal pathology in Alzheimer's disease. I. Ganglion cell loss in foveal/parafoveal retina. Neurobiol. Aging. 1996b; 17:377–384. [PubMed: 8725899]

Buckner RL, Head D, Parker J, Fotenos AF, Marcus D, Morris JC, Snyder AZ. A unified approach for morphometric and functional data analysis in young, old, and demented adults using automated atlas-based head size normalization: reliability and validation against manual measurement of total intracranial volume. Neuroimage. 2004; 3:724–738.

Caselli RJ, Locke DE, Dueck AC, Knopman DS, Woodruff BK, Hoffman-Snyder C, Rademakers R, Fleisher AS, Reiman EM. The neuropsychology of normal aging and preclinical Alzheimer's disease. Alzheimers Dement. 2014; 10:84–92. [PubMed: 23541188]

Dale AM, Fischl B, Sereno MI. Cortical surface-based analysis. I. Segmentation and surface reconstruction. Neuroimage. 1999; 9:179–194. [PubMed: 9931268]

Delis, DC., Kramer, JH., Kaplan, E., Ober, BA. California Verbal Learning Test: Adult Version. Manual. Psychological Corportation; San Antonia, TX: 1987.

Delis, DC., Kramer, JH., Kaplan, E., Ober, BA. Adult Version. Manual. Psychological Corporation; San Antonio, TX: 2000. California Verbal Learning Test- Second Edition.

Fischl B, Liu A, Dale AM. Automated manifold surgery: constructing geometrically accurate and topologically correct models of the human cerebral cortex. IEEE Trans. Med. Imaging. 2001; 20:70–80. [PubMed: 11293693]

Fischl B, Sereno MI, Dale AM. Cortical surface-based analysis. II. inflation, flattening, and a surface-based coordinate system. Neuroimage. 1999; 9:195–207. [PubMed: 9931269]

Garcia-Martin E, Bambo MP, Marques ML, Satue M, Otin S, Larrosa JM, Polo V, Pablo LE. Ganglion cell layer measurements correlate with disease severity in patients with Alzheimer's disease. Acta Ophthalmol. 2016; 94:e454–e459. [PubMed: 26895692]

Gelfand JM, Goodin DS, Boscardin WJ, Nolan R, Cuneo A, Green AJ. Retinal axonal loss begins early in the course of multiple sclerosis and is similar between progressive phenotypes. PLoS One. 2012; 7:e36847. [PubMed: 22666330]

Hafler BP, Klein ZA, Jimmy Zhou Z, Strittmatter SM. Progressive retinal degeneration and accumulation of autofluorescent lipopigments in Progranulin deficient mice. Brain Res. 2014; 1588:168–174. [PubMed: 25234724]

Helmer C, Malet F, Rougier MB, Schweitzer C, Colin J, Delyfer MN, Korobelnik JF, Barberger-Gateau P, Dartigues JF, Delcourt C. Is there a link between open-angle glaucoma and dementia? The Three-City-Alienor cohort. Ann. Neurol. 2013; 74:171–179. [PubMed: 23686609]

Hinton DR, Sadun AA, Blanks JC, Miller CA. Optic-nerve degeneration in Alzheimer's disease. N. Engl. J. Med. 1986; 315:485–487. [PubMed: 3736630]

Jack CR Jr, Knopman DS, Jagust WJ, Petersen RC, Weiner MW, Aisen PS, Shaw LM, Vemuri P, Wiste HJ, Weigand SD, Lesnick TG, Pankratz VS, Donohue MC, Trojanowski JQ. Tracking

pathophysiological processes in Alzheimer's disease: an updated hypothetical model of dynamic biomarkers. Lancet Neurol. 2013; 12:207–216. [PubMed: 23332364]

Kirwan CB, Hartshorn A, Stark SM, Goodrich-Hunsaker NJ, Hopkins RO, Stark CEL. Pattern separation deficits following damage to the hippocampus. Neuropsychologia. 2012; 50:2408–2414. [PubMed: 22732491]

Kirwan CB, Stark CE. Overcoming interference: an fMRI investigation of pattern separation in the medial temporal lobe. Learn Mem. 2007; 14:625–633. [PubMed: 17848502]

Koronyo-Hamaoui M, Koronyo Y, Ljubimov AV, Miller CA, Ko MK, Black KL, Schwartz M, Farkas DL. Identification of amyloid plaques in retinas from Alzheimer's patients and noninvasive in vivo optical imaging of retinal plaques in a mouse model. Neuroimage. 2011; 54(Suppl 1):S204–S217. [PubMed: 20550967]

Law JR, Flanery MA, Wirth S, Yanike M, Smith AC, Frank LM, Suzuki WA, Brown EN, Stark CE. Functional magnetic resonance imaging activity during the gradual acquisition and expression of paired-associate memory. J. Neurosci. 2005; 25:5720–5729. [PubMed: 15958738]

Lu Y, He HJ, Zhou J, Miao JY, Lu J, He YG, Pan R, Wei Y, Liu Y, He RQ. Hyperphosphorylation results in tau dysfunction in DNA folding and protection. J. Alzheimers Dis. 2013; 37:551–563. [PubMed: 24064506]

McKhann GM, Knopman DS, Chertkow H, Hyman BT, Jack CR Jr, Kawas CH, Klunk WE, Koroshetz WJ, Manly JJ, Mayeux R, Mohs RC, Morris JC, Rossor MN, Scheltens P, Carrillo MC, Thies B, Weintraub S, Phelps CH. The diagnosis of dementia due to Alzheimer's disease: recommendations from the National Institute on Aging-Alzheimer's Association workgroups on diagnostic guidelines for Alzheimer's disease. Alzheimers Dement. 2011; 7:263–269. [PubMed: 21514250]

Ong YT, Hilal S, Cheung CY, Venketasubramanian N, Niessen WJ, Vrooman H, Anuar AR, Chew M, Chen C, Wong TY, Ikram MK. Retinal neurodegeneration on optical coherence tomography and cerebral atrophy. Neurosci. Lett. 2015; 584:12–16. [PubMed: 25451722]

Paquet C, Boissonnot M, Roger F, Dighiero P, Gil R, Hugon J. Abnormal retinal thickness in patients with mild cognitive impairment and Alzheimer's disease. Neurosci. Lett. 2007; 420:97–99. [PubMed: 17543991]

Perez SE, Lumayag S, Kovacs B, Mufson EJ, Xu S. Beta-amyloid deposition and functional impairment in the retina of the APPswe/PS1DeltaE9 transgenic mouse model of Alzheimer's disease. Invest. Ophthalmol. Vis. Sci. 2009; 50:793–800. [PubMed: 18791173]

Rabinovici GD, Seeley WW, Kim EJ, Gorno-Tempini ML, Rascovsky K, Pagliaro TA, Allison SC, Halabi C, Kramer JH, Johnson JK, Weiner MW, Forman MS, Trojanowski JQ, Dearmond SJ, Miller BL, Rosen HJ. Distinct MRI atrophy patterns in autopsy-proven Alzheimer's disease and frontotemporal lobar degeneration. Am. J. Alzheimers Dis. Other Demen. 2007; 22:474–488.

Schacter DL. The seven sins of memory. Insights from psychology and cognitive neuroscience. Am. Psychol. 1999; 54:182–203. [PubMed: 10199218]

Schon C, Hoffmann NA, Ochs SM, Burgold S, Filser S, Steinbach S, Seeliger MW, Arzberger T, Goedert M, Kretzschmar HA, Schmidt B, Herms J. Long-term in vivo imaging of fibrillar tau in the retina of P301S transgenic mice. PLoS One. 2012; 7:e53547. [PubMed: 23300938]

Segonne F, Dale AM, Busa E, Glessner M, Salat D, Hahn HK, Fischl B. A hybrid approach to the skull stripping problem in MRI. Neuroimage. 2004; 22:1060–1075. [PubMed: 15219578]

Sivak JM. The aging eye: common degenerative mechanisms between the Alzheimer's brain and retinal disease. Invest. Ophthalmol. Vis. Sci. 2013; 54:871–880. [PubMed: 23364356]

Squire LR. Memory systems of the brain: a brief history and current perspective. Neurobiol. Learn Mem. 2004; 82:171–177. [PubMed: 15464402]

Squire LR, Stark CE, Clark RE. The medial temporal lobe. Annu. Rev. Neurosci. 2004; 27:279–306. [PubMed: 15217334]

Stark SM, Yassa MA, Lacy JW, Stark CE. A task to assess behavioral pattern separation (BPS) in humans: data from healthy aging and mild cognitive impairment. Neuropsychologia. 2013; 51:2442–2449. [PubMed: 23313292]

Szigeti A, Tátrai E, Varga BE, Szamosi A, DeBuc DC, Nagy ZZ, Németh J, Somfai GM. The effect of axial length on the thickness of intraretinal layers of the macula. PLoS One. 2015; 10:e0142383. [PubMed: 26544553]

Tamura H, Kawakami H, Kanamoto T, Kato T, Yokoyama T, Sasaki K, Izumi Y, Matsumoto M, Mishima HK. High frequency of open-angle glaucoma in Japanese patients with Alzheimer's disease. J. Neurol. Sci. 2006; 246:79–83. [PubMed: 16564058]

Ward ME, Taubes A, Chen R, Miller BL, Sephton CF, Gelfand JM, Minami S, Boscardin J, Martens LH, Seeley WW, Yu G, Herz J, Filiano AJ, Arrant AE, Roberson ED, Kraft TW, Farese RV Jr, Green A, Gan L. Early retinal neurodegeneration and impaired Ran-mediated nuclear import of TDP-43 in progranulin-deficient FTLD. J. Exp. Med. 2014; 211:1937–1945. [PubMed: 25155018]

Yassa MA, Lacy JW, Stark SM, Albert MS, Gallagher M, Stark CE. Pattern separation deficits associated with increased hippocampal CA3 and dentate gyrus activity in nondemented older adults. Hippocampus. 2011; 21:968–979. [PubMed: 20865732]

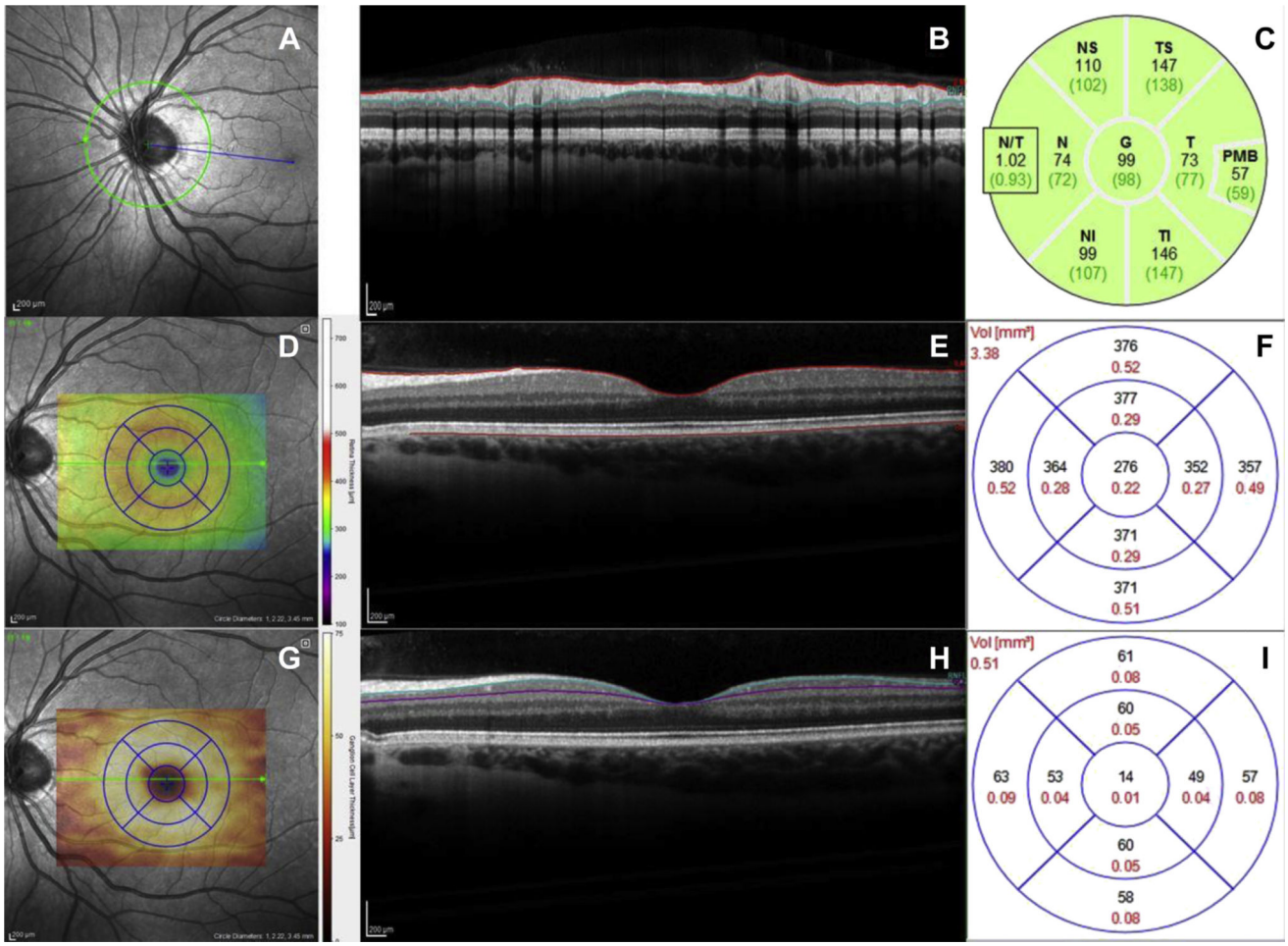

Fig. 1.

(A) Fundus image of the retina centered on the optic nerve head. The green circle specifies the location of a peripapillary retinal nerve fiber layer (RNFL) OCT scan consisting of 1 circular B-scan. (B) Cross-sectional OCT image of B-scan outlined in panel A. Red and blue lines delineate the thickness of the RNFL, the layer of axons connecting retinal ganglion cells to the brain. (C) Thickness map evaluating RNFL thickness in microns from scan in panel B. The global thickness value found in the center of the map was used in our analyses. (D) Fundus image of the macula. Blue 1-, 2.22-, and 3.45-mm grid centered on the fovea indicates area in which thickness and volume values were calculated. (E) Cross-sectional OCT image of a horizontal B-scan taken through the fovea. Red lines outline the area measured to calculate macular thicknesses. (F) Grid corresponding to that in panel D with thickness values in microns for each sector. Thickness values from 19 B-scans were integrated to evaluate total macular volume. (G, H, and I). Same macular fundus photo and OCT scan as in panels D and E, segmented for the ganglion cell layer (GCL). Blue and purple lines outline the macular GCL, and the grid in panel I indicates sector values for GCL thickness in microns. Abbreviation: OCT, optical coherence tomography. (For interpretation of the references to color in this figure legend, the reader is referred to the Web version of this article.)

Table 1

Clinical and demographic characteristics of neurologically normal older adults (n = 79); mean and standard deviation presented unless otherwise specified

Clinical and demographic variable	Value
Demographics	
Age, y	76.0 (5.5)
Education, y	17.6 (2.0)
Sex, %F, n	53.3 (42)
Cognition	
MMSE (median, interquartile range)	29.5 (28, 30)
CVLT-II long delay free recall (median, interquartile range)	13.0 (11, 15)
Behavioral Pattern Separation Test	
Percent correct	68.5 (6.03)
Response bias	26.2 (21.0)
Retinal structure	
Total avg peripapillary RNFL thickness (μm)	89.5 (12.3)
Superior	109.2 (16.3)
Inferior	114.6 (20.0)
Temporal	66.6 (11.8)
Nasal	70.6 (16.0)
Total avg macular volume (mm^3)	3.0 (0.1)
Total avg macular ganglion cell volume (mm^3)	0.40 (0.04)
Neuroanatomic volumes (mm^3)	
Medial temporal lobes	15,204.9 (1619.9)
Parahippocampal	4173.6 (549.2)
Entorhinal	3691.2 (693.1)
Hippocampal	7341.1 (833.6)
Temporoparietal	46,561.6 (4650.8)
Posterior cingulate	6112.3 (791.8)
Precuneus	18,154.2 (1833.4)
Middle frontal	39,209.0 (5339.9)
Primary motor	24,845.5 (2948.2)
Basal ganglia	20,784.3 (2284.5)

Key: avg, average; CVLT-II, California Verbal Learning Test-second edition; MMSE, mini-mental state examination; RNFL, retinal nerve fiber layer.

Table 2

Multivariable linear regression models demonstrating associations between retinal structure and medial temporal lobe volumes among neurologically normal older adults (n = 79)

Outcome: medial temporal lobe volume			
Variable	**β**	**b**	**95% CI**
Retinal nerve fiber layer (RNFL) thickness (μm)			
Age	−0.30	−93.2	−159.0, −27.4
Sex	−0.11	−352.3	−1252.7, 548.1
TIV	0.50	0.005	0.002, 0.008
RNFL Thickness	0.31	39.3	11.9, 66.8
Model adj. $R^2 = 0.34$			
Total macular volume (mm^3)			
Age	−0.24	−76.9	−144.6, −9.1
Sex	0.05	172.7	−809.9, 1155.3
TIV	0.57	0.006	0.003, 0.009
Macular volume	0.23	3013.6	59.4, 5967.8
Model adj. $R^2 = 0.31$			
Macular ganglion volume (mm^3)			
Age	−0.20	−65.1	−133.4, 3.4
Sex	0.02	61.2	−889.6, 1012.1
TIV	0.57	0.005	0.003, 0.009
Macular ganglion volume	0.30	12,590.4	3249.4, 21,931.5
Model adj. $R^2 = 0.33$			

Key: adj., adjusted; TIV, total intracranial volume.